Journal of Neurochemistry

JOURNAL OF NEUROCHEMISTRY | 2019 | 150 | 188–201 doi: 10.1111/jnc.14681



ORIGINAL ARTICLE

# PET imaging of dopamine release in the frontal cortex of manganese-exposed non-human primates

Tomas R. Guilarte*† , Chien-Lin Yeh‡§, Jennifer L. McGlothan*, Juan Perez*, Paige Finley†, Yun Zhou†, Dean F. Wong†, Ulrike Dydak‡§ and Jay S. Schneider¶

*Department of Environmental Health Sciences, Robert Stempel College of Public Health and Social Work, Florida International University, Miami, Florida, USA

†Department of Radiology, Johns Hopkins Medical Institutions, Baltimore, Maryland, USA

‡Department of Radiology and Imaging Sciences, Indiana University School of Medicine, Indianapolis, Indiana, USA

§School of Health Sciences, Purdue University, West Lafayette, Indiana, USA

¶Department of Pathology, Anatomy & Cell Biology, Thomas Jefferson University, Philadelphia, Pennsylvania, USA

**Abstract**

Humans and non-human primates exposed to excess levels of manganese (Mn) exhibit deficits in working memory and attention. Frontal cortex and fronto-striatal networks are implicated in working memory and these circuits rely on dopamine for optimal performance. Here, we aimed to determine if chronic Mn exposure alters *in vivo* dopamine release (DAR) in the frontal cortex of non-human primates. We used [$^{11}$C]-FLB457 positron emission tomography with amphetamine challenge to measure DAR in *Cynomolgus macaques*. Animals received [$^{11}$C]-FLB457 positron emission tomography scans with and without amphetamine challenge prior to Mn exposure (baseline), at different time points during the Mn exposure period, and after 10 months of Mn exposure cessation. Four of six Mn-exposed animals expressed significant impairment of frontal cortex *in vivo* DAR relative to baseline. One Mn animal had no change in DAR and another Mn animal expressed increased DAR relative to baseline. In the reversal studies, one Mn-exposed animal exhibited complete recovery of DAR while the second animal had partial recovery. In both animals, frontal cortex Mn concentrations normalized after 10 months of exposure cessation based on T1-weighted magnetic resonance imaging. D1-dopamine receptor (D1R) autoradiography in frontal cortex tissue indicates that Mn animals that experienced cessation of Mn exposure expressed D1R levels that were approximately 50% lower than Mn animals that did not experience cessation of Mn exposure or control animals. The present study provides evidence of Mn-induced alterations in frontal cortex DAR and D1R that may be associated with working memory and attention deficits observed in Mn-exposed subjects.

**Keywords:** [$^{11}$C]-FLB457 PET, attention, dopamine, frontal cortex, manganese, working memory.

*J. Neurochem.* (2019) **150**, 188–201.

Received April 6, 2018; revised manuscript received June 22, 2018; January 30, 2019; accepted February 1, 2019.

Address correspondence and reprint requests to Prof. Tomás R. Guilarte, Environmental Health Sciences, Cognitive Neuroscience & Imaging, Robert Stempel College of Public Health and Social Work, Florida International University, 11200 SW 8th Street, AHC5-507, Miami, FL 33199, USA. E-mail: tguilart@fiu.edu

*Abbreviations used*: 5-CSRT, 5-choice serial reaction time; AMPH, amphetamine; D1R, D1 dopamine receptor; D2R, D2 dopamine receptor; DAR, dopamine release; Hep/dex, heparin/dextrose; i.v., intravenous; Mn, manganese; MRI, magnetic resonance imaging; PET, positron emission tomography; ROI, regions of interest; SNpc, substantia nigra pars compacta.



 

Exposure to excess levels of manganese (Mn) from a variety of sources results in increased brain Mn concentrations and neurological deficits including parkinsonism with dystonia, cognitive deficits, and psychiatric abnormalities (Pal *et al.* 1999; Olanow 2004; Perl and Olanow 2007; Guilarte 2010, 2013; Guilarte and Gonzales 2015; Mackenzie Ross 2018). The clinical expression of exposure to high levels of Mn in humans appears to be a continuum with different clinical manifestations beginning with psychosis and cognitive function deficits followed by parkinsonian-like movement abnormalities that are most likely caused by effects on different neuronal systems and brain regions (Mergler *et al.* 1999; Guilarte 2010, 2013).

The current knowledge of the cognitive deficits and underlying neurobiology associated with chronic Mn exposure is limited, but several studies indicate that humans with increased exposure to Mn express impairments in attention and working memory indicative of frontal lobe and subcortical dysfunction (Mirowitz *et al.* 1991; Bowler *et al.* 2003, 2006, 2007a,b; Josephs *et al.* 2005; Klos *et al.* 2006; Park *et al.* 2009; Guilarte 2010, 2013; Guilarte and Gonzales 2015; Mackenzie Ross 2018). Workers occupationally exposed to Mn also have a high incidence of neuropsychiatric symptoms and increased brain Mn concentrations affect working memory performance (Bowler *et al.* 2003, 2006, 2007a,b; Klos *et al.* 2006; Bouchard *et al.* 2007; Chalela *et al.* 2010) and result in poor cognitive function (Mergler and Baldwin 1997; Santos-Burgoa *et al.* 2001; Bowler *et al.* 2003, 2007a,b; Klos *et al.* 2006; Chalela *et al.* 2010; Roels *et al.* 2013).

Studies in different species from rodents to non-human primates and humans have shown that working memory is closely associated with frontal cortex and fronto-striatal circuits (Constantinidis and Wang 2004; Linden 2007). Dopaminergic innervation of the striatum (Rinne *et al.* 2000; Sawamoto *et al.* 2008; Jokinen *et al.* 2013) and frontal cortex (Brozoski *et al.* 1979; Aalto *et al.* 2005; Rotaru *et al.* 2007) are important for working memory and attention. Dopaminergic neurons from the substantia nigra pars compacta innervate the striatum and are primarily involved in the execution and control of movement. On the other hand, mesocortical dopaminergic neuron innervation of the frontal cortex from the ventral tegmental area is involved in cognitive function including working memory (Bjorklund and Dunnett 2007). The caudate nucleus also receives dopaminergic input from the substantia nigra pars compacta that interacts with the frontal cortex via fronto-striatal circuits (Alexander *et al.* 1986; Seger 2006). The dorsolateral prefrontal cortex is an important brain region for the execution of working memory and attentional processes with reciprocal connections to other cortical structures such as the parietal, temporal, and cingulate cortex that comprise the working memory cortical network (Petrides *et al.* 1993; Berman *et al.* 1995; Cohen *et al.* 1997). The aim of our present studies was to examine the effects of chronic Mn exposure on *in vivo* frontal cortex dopamine release (DAR) using positron emission tomography (PET) in order to understand the potential role of the dopaminergic system in the underlying neurobiology of Mn-induced working memory and attention deficits.

The ability to non-invasively measure chemistry changes in the living brain has been critically important in understanding the role of neurotransmitter systems on cognitive function. The competitive displacement of a reversible D2-dopamine receptor (D2R)-specific PET ligand such as [$^{11}$C]-raclopride by endogenous dopamine released from axonal terminals following an acute amphetamine (AMPH) challenge has been validated and used extensively to measure *in vivo* dopamine release (DAR) in the striatum (Laruelle 2000; Guilarte *et al.* 2006, 2008a) and in the frontal cortex (Narendran *et al.* 2009, 2011a,b, 2014). The level of dopaminergic innervation to the frontal cortex is significantly less than to the striatum; thus, it is more difficult to assess *in vivo* DAR by PET in the frontal cortex than in the striatum and the ligands used for estimating DAR in the striatum are not feasible to use in extra-striatal regions. However, the availability of high-affinity D2R-PET ligands such as [$^{11}$C]-FLB457 ($K_d$ = 0.06 nM) has made extra-striatal DAR studies possible in humans and non-human primates. Several studies have now described the reliability of using [$^{11}$C]-FLB457 PET with AMPH challenge to measure *in vivo* DAR in the frontal cortex of humans and non-human primates (Narendran *et al.* 2009, 2011a,b, 2014). Further, the degree of reduction of [$^{11}$C]-FLB457 binding potential measured by PET has been shown to be directly associated with the amount of extracellular DAR induced by an acute AMPH administration (Jedema *et al.* 2014; Narendran *et al.* 2014).

Previous studies from our laboratory have shown that non-human primates chronically exposed to Mn express deficits in working memory and attention (Schneider *et al.* 2006, 2009, 2015). We have also shown that chronic Mn exposure produces a marked inhibition of *in vivo* DAR in the striatum measured by [$^{11}$C]-raclopride PET with AMPH challenge (Guilarte *et al.* 2006, 2008a). Based on this knowledge, we aimed to determine if non-human primates exposed to a chronic Mn administration paradigm that results in working memory and attention deficits (Schneider *et al.* 2015) exhibit disruption of *in vivo* DAR in the frontal cortex measured by [$^{11}$C]-FLB457 PET with AMPH challenge. We also tested in two of the Mn-exposed animals the possibility that cessation of Mn exposure may reverse the effects of Mn on frontal cortex DAR and determined the time for elimination of frontal cortex Mn using T1-weighted magnetic resonance imaging (MRI).

## Materials and methods

This study was not pre-registered.

### Study design and Mn administration

Animals used in this study were obtained from SNBL (Everett, WA, USA) Ltd. (Mn1–Mn7) and Primate Products, Inc. (Immokalee, FL, USA) (Mn9-Mn14). Age and weight of the animals are shown in Table 1. All animals were single housed in standard cages and during cognitive training/testing sessions were maintained on a food restriction schedule and water was provided *ad libitum*. Six young adult male research naive *Cynomolgus macaques* (*macaca fascicularis*) were used for the neuroimaging part of this study. No power calculations for the number of animals were done for this study as we used all available animals in which neuroimaging was performed. Behavioral assessment of these animals has been described by us previously (Schneider *et al.* 2015). While this previous publication described nine Mn-exposed animals, we were only able to perform neuroimaging studies in six of the nine Mn-exposed animals.

All animal studies were reviewed and approved by the Columbia University, Johns Hopkins University, and Thomas Jefferson University Animal Care and Use Committees. Animals were received from the supplier and housed at Thomas Jefferson University where they were quarantined. Following the release from quarantine, animals began to learn the various behavioral tasks until their learning performance reached the criteria. Animals that learned the behavioral tasks to criteria first were immediately utilized in the study. That is, they received baseline neuroimaging studies and began chronic administration of Mn.

#### *Imaging studies*

Animals were transferred from Thomas Jefferson University to the Johns Hopkins Hospital for baseline imaging studies prior to starting Mn dosing. Upon their return to Thomas Jefferson University, animals (Mn1, Mn3, Mn4, and Mn6) were anesthetized and underwent a surgical procedure for placement of an indwelling jugular catheter attached to a titanium vascular access port secured to muscle parallel to the thoracic spine (MIDA-CBAS-C50; Instech Laboratories, Inc., Plymouth Meeting, PA, USA). Following an approximate 2-week post-surgery recovery period, behavioral testing was reinitiated and once a stable level of performance was confirmed, Mn exposure was initiated. For access to the ports, skin overlying the port was shaved and disinfected with DuraPrep Surgical Solution (3M; St. Paul, MN, USA). Ports were flushed at least once per week prior to initiation of Mn exposure. Using aseptic technique, a Huber needle, attached to a syringe, was inserted through the skin into the septum of the port. Saline (approx. 3.0 mL) was infused to verify patency of the catheter and then the line was locked with heparin/dextrose locking solution (hep/dex, 0.3 mL heparin (10 000 U/mL in 3 mL dextrose). For Mn administration, after an initial saline flush, the syringe was removed and replaced with one containing Mn solution (or saline vehicle). Mn was infused at a rate of approximately 0.5 mL/min. followed by a flush of approximately 3.0–5.0 mL of sterile saline and hep/dex locking solution. In order to minimize risk of injuries to staff and animals and minimize animal stress, the port was accessed while the animals were seated in a chair and under light gas sedation (isofluorane 4% to induce, 2% to maintain, and oxygen 1%).

Administration of Mn as manganese sulfate monohydrate ($MnSO_4$ monohydrate; Sigma-Aldrich, St. Louis, MO, USA) was used as follows: 15 mg/kg/week for 5 weeks and then 20 mg/kg/week for the remainder of the study period with the total dose per week was divided and given at two different times/week. Manganese sulfate was prepared fresh for each injection (50 mg/mL in sterile saline), pH adjusted to 7.0, filtered, and warmed to 37°C prior to use. Although all animals were implanted with vascular access ports for administration of Mn, these ports failed in all animals and were removed surgically. Following, removal of ports, Mn or vehicle was administered intravenously by slow infusion (rate of

**Table 1** Dosing schedule and cumulative doses administered to individual animals

| | | | Mn-1 | | | Mn-2 | | |
|---|---|---|---|---|---|---|---|---|
| ID | Age (yrs) | Weight (kg) | Exposure duration (weeks) | Cumulative Mn (mg/kg BW) | Cumulative Mn (mg) | Exposure duration (weeks) | Cumulative Mn (mg/kg BW) | Cumulative Mn (mg) |
| Mn2 | 8.7 | 7.8 | 33 | 0 | 0 | 78 | 0 | 0 |
| Mn5 | 9.0 | 6.6 | 61 | 0 | 0 | 78 | 0 | 0 |
| Mn7 | 8.9 | 5.9 | 56 | 0 | 0 | 78 | 0 | 0 |
| Mn13 | 8.8 | 8.4 | – | – | – | – | – | – |
| Mn14 | 8.7 | 8.0 | – | – | – | – | – | – |
| Mn1 | 8.6 | 5.9 | 41 | 258.3 | 1568.2 | 80 | 511.9 | 3135.7 |
| Mn3[a] | 9.8 | 7.8 | 33 | 206.4 | 1216.0 | 80 | 512.0 | 3215.4 |
| Mn4 | 10.3 | 8.1 | 26 | 214.0 | 1687.3 | 81 | 517.2 | 4292.7 |
| Mn6[a] | 9.3 | 8.6 | 27 | 219.4 | 1779.6 | 66 | 421.0 | 3335.2 |
| Mn9 | 10.0 | 7.5 | + | + | + | 60 | 382.0 | 3065.8 |
| Mn11 | 9.8 | 8.6 | + | + | + | 60 | 375.5 | 3193.3 |

Each animal received saline or 15–20 mg/kg of $MnSO_4$ (5–6.7 mg/kg BW of Mn) per week. This weekly dose was split and administered on two different occasions per week.

[a]These animals underwent an additional imaging set 44 weeks after removal from Mn exposure to monitor any reversal of Mn-induced effects. + positron emission tomography and magnetic resonance imaging was not performed at Mn-1.

0.5 mL/min over a 4–6 min period), under the same anesthesia conditions used for port access. After dosing, animals are returned to their home cage and observed for any adverse events. At the first imaging time point after initiation of Mn exposure (Mn-1) and the second imaging time point (Mn-2) or at 10 months after the cessation of Mn administration (reversal), animals received the same imaging studies as in baseline. Animals were killed by ketamine injection (20–30 mg/kg) followed by an overdose of pentobarbital (100 mg/kg) and the brain was harvested as previously described (Guilarte *et al.* 2008a,b).

### *Behavioral studies*

The procedures to assess attention and working memory performance in these animals have been described by us previously (Schneider *et al.* 2015). Animals were adapted to sitting in a primate chair and trained to perform various behavioral tasks in an automated panel using the non-human primate Cambridge Neuropsychological Test Automated Battery (CANTAB) and the CANTAB Intellistation with pellet reward (Lafayette Neuroscience, Lafayette, IN, USA).

*Attention.* The 5-choice serial reaction time was used to assess attention. As described by us previously (Schneider *et al.* 2015); "the test involves training the animals to respond to a brief visual stimulus presented in an unpredictable fashion in one of five locations on a touch screen. On this version of the test, the animal depresses a bar for 2 s and is presented with a set of five empty target stimuli (five empty circles) on the screen. One of the five circles turns yellow 0.5–1 s after the circles appear on the screen. Once a circle turns yellow, the animal has to touch it as soon as possible and a touch of the circle within the allotted time of 5 s maximum is scored as a correct response and reinforced. Each session consists of 100 trials."

*Working memory.* We used the self-ordered spatial search task to determine the effect of chronic Mn exposure on working memory as described by us previously (Schneider *et al.* 2015). "This task requires the animal to touch identical squares located in different spatial locations in a self-ordered sequence without returning to a previously touched square. The task has three levels of difficulty. At the easiest level, two blue boxes appear randomly on the screen in 16 possible locations and in no obvious pattern. For successful completion of the task, subjects have to remember the location of each box and touch all boxes without revisiting a box once it has been touched. After a touch, the screen blanks for 2 s and then the boxes reappear in the same locations as before. The animal needs to remember which box it previously touched and now touches the other one. If the animal touches the box that previously was not touched, it receives a reward. However, if it touches the same box as previously touched, no reward is given and the boxes disappear from the screen for a 20 s time-out period. If the animal touches all of the boxes in sequence without a repetition, the trial is labeled correct. Once the two boxes trials are achieved, the animal is introduced to a higher degree of difficulty with three and four boxes. A testing session consists of 40 trials grouped into blocks by trial type: 2, 3, and 4 boxes. Accuracy (percent correct responses) were calculated for each trial type by dividing the number of correctly completed trials by the number of trials in which there were at least one response."(Schneider *et al.* 2015).

## [$^{11}$C]-FLB 457 positron emission tomography with amphetamine challenge

Animals were fasted for 12 hrs prior to the imaging studies and were initially anesthetized by an intramuscular injection of ketamine (20–30 mg/kg). During the imaging study, one i.v. catheter was implanted to maintain anesthesia throughout the study by a continuous i.v. infusion drip of ~ 122 μg/kg/min of Propofol. An additional i.v. catheter was placed to keep an open vein for injection of the [$^{11}$C]-FLB 457 tracer. In addition, all animals were intubated to keep an open airway, and pulse and oxygen saturation were continuously monitored during the studies until the animal was awake and returned to normal activity. Each PET session consisted of two [$^{11}$C]-FLB 457 scans performed in a GE Advance 3D PET scanner with approximately 70 min in between scans. For the PET study, animals were secured to the PET table using an individually fitted thermoplastic mask attached to a head holder, which allows reproducible positioning between studies. Once positioned in the PET scanner, a transmission scan was performed on the animal with a 10 mCi $^{68}$ Ga source to allow for attenuation correction. PET scanning was started immediately after i.v. injection of [$^{11}$C]-FLB457. All animals received two 90-min dynamic [$^{11}$C]-FLB 457 PET scans with approximately 70 min between scans. The first scan was with no AMPH administered prior to the injection of [$^{11}$C]-FLB457. The second scan was the Post-AMPH scan, where 2 mg/kg body weight of AMPH was administered 5 min prior to the [$^{11}$C]-FLB 457 injection. This was done to measure AMPH-induced DAR. Regions of interest (ROIs) included the frontal cortex and cerebellum (the latter was used as a reference region for the measurement of free and nonspecific binding) and were manually drawn on blinded PET images co-registered with MRI images of the same animal. A simplified reference tissue model and linear regression with spatial constraint algorithm were used to generate binding potential ($BP_{ND}$) images (Zhou *et al.* 2003, 2006). ROI $BP_{ND}$ was obtained by applying ROI to $BP_{ND}$ images. %DAR was calculated as: %DAR = (($BP_{ND}$ AMPH/$BP_{ND}$ Saline) − 1) * 100.

## T1-weighted MRI procedures

Structural images and relaxometric data were acquired using a 3T Philips Achieva MRI scanner using an 8-channel receiver/transmitter knee coil. High-resolution 3D T1-weighted images were obtained using a fast gradient echo pulse sequence with repetition time (TR) = 25 ms, echo time = 3.85 ms, slice thickness 1.5 mm, 0.75 mm slice gap, and in-plane resolution (pixel size) of 0.5 × 0.5 mm$^2$ as anatomical reference. A total of 75 slices were collected. To assess changes of the T1 relaxation time, inversion recovery fast spin echo images were acquired using seven different inversion times (Ti) for quantifying Mn accumulation in the brain collected with TR/echo time = 4000/13.7 ms and Ti = 100, 300, 500, 700, 1000, 1500, 3000 ms. Up to 18 slices with thickness 2.2 mm were acquired with field of view 160 × 160 mm$^2$ and matrix size 160 × 160. Images were reconstructed to a 320 × 320 matrix, resulting in in-plane resolution of 0.5 × 0.5 mm$^2$. Total scan time for seven inversion recovery images were 16 min and 3 s.

## T1 relaxation time calculation

The T1 relaxation time for each pixel was then calculated by the least-squares method in Matlab (The Mathworks, Natrick, MA, USA) (RRID:SCR_001622) using the following equation for T1:

$$S = S0 * [1 - f * \exp(-\mathrm{Ti}/\mathrm{T1}) + \exp(-\mathrm{TR}/\mathrm{T1})]$$

where $S$ = measured signal intensity, $S0$ = signal without any T1 contrast = proton density signal, Ti = inversion time, T1 = relaxation time, TR = repetition time, $f$ = inversion factor.

Using seven different inversion times Ti, the respective signal (S), and the known TR yield a system of equations that was solved by the least square fitting to obtain results for f, SO, and the T1 relaxation time for each pixel.

To obtain an average frontal lobe T1 relaxation time, ROIs of 2.5 $mm^2$ in diameter were placed bilaterally in frontal gray matter and the T1 values were then averaged over the two ROIs.

#### *Quantitative autoradiography of D1R receptors*

We followed the same protocol previously used in our lab to visualize and measure the distribution of D1-dopamine receptor (D1R) in the striatum (Guilarte *et al.* 2008a). Briefly, frozen sections were thawed on a slide warmer for 30 min at 37°C. The slides were then pre-incubated at 20–25°C for 20 min in buffer (50 mM Tris HCl, pH 7.4 with 120 mM NaCl, 5 mM KCl, 2 mM $CaCl_2$, and 1 mM $MgCl_2$). D1R was then labeled at 20–25°C with 1 nM [$^3$H]-SCH23390 (specific activity: 81.9 Ci/mmol; Perkin Elmer, Waltham, MA, USA) in buffer (50 mM Tris HCl, pH 7.4 with 120 mM NaCl, 5 mM KCl, 2 mM $CaCl_2$, 1 mM $MgCl_2$, and 1 mM Ascorbic Acid) for 30 min. Nonspecific binding was assessed in adjacent sections with the addition of non-radioactive 5 μM (+)-butaclamol (Sigma-Aldrich). In order to block any [$^3$H]-SCH23390 binding to serotonin receptors, all test tubes contained the addition of 40 nM of ketanserin (Sigma-Aldrich) just prior to the assay. Sections were then rinsed five times in buffer (50 mM Tris HCl, pH 7.4 with 120 mM NaCl, 5 mM KCl, 2 mM $CaCl_2$, 1 mM $MgCl_2$, and 1 mM Ascorbic Acid) at 4°C for 20 s each. The slides were dipped in $dH_2O$ and dried overnight. Sections were apposed to Kodak Bio-Max MR films with tritium microscales for 6 weeks (GE Healthcare, Piscataway, NJ, USA). Images were acquired and quantified in a blinded fashion using the MCID software (InterFocus Imaging Ltd., Cambridge, UK). (RRID: SCR_014419).

### Statistics

All analysis of imaging data, behavioral data, and autoradiography data was performed by a person blinded to the current animal identifier and time point in the study. Data for PET DAR and MRI T1 relaxation times were analyzed using repeated measures analysis of variance (ANOVA) with Bonferroni correction for multiple comparisons. Mean imputation was used for missing 8-month imaging data (Mn9 and Mn11). Behavioral data failed normality tests, therefore were analyzed by a nonparametric Friedman's ANOVA. A sample *t*-test with Bonferroni adjustment was applied for multiple comparisons. For autoradiography studies, control and Mn-exposed results were compared using *t*-test. Mn + reversal data are presented as two observations and were not included in statistical analysis. Statistical significance was defined at $p < 0.05$ (Bonferroni correction $p < 0.017$). Normality of data was assessed using Shapiro–Wilk test for small sample sizes. For data that do not pass sphericity test, a Greenhouse-Geisser correction is applied. Statistical analysis was performed using IBM SPSS Statistics 20 software (Armonk, NY, USA) (RRID: SCR_002865).

## Results

### Manganese dosing paradigm

In Table 1, we describe the level of Mn exposure, time of exposure, and cumulative Mn doses in total absolute amount administered and also based on body weight. This dosing paradigm was selected because it results in blood Mn concentrations in the upper range of levels that have been described in non-occupationally exposed populations (Guilarte *et al.* 2006, 2008a). Further, this Mn dose level is well tolerated by the animals and we have previously shown that it produces deficits in behavioral tests of motor and cognitive function (Schneider *et al.* 2006, 2009, 2013, 2015) as well as *in vivo* DAR in the striatum (Guilarte *et al.* 2006, 2008a).

### [$^{11}$C]-FLB457 PET with AMPH challenge and T1-weighted MRI in the frontal cortex of Mn-exposed animals

We used a total of six Mn-exposed animals to perform *in vivo* frontal cortex DAR studies measured by [$^{11}$C]-FLB457 PET with AMPH challenge. In Fig. 1, we show the results for one of the animals (Mn3) that received [$^{11}$C]-FLB457 PET with AMPH challenge at three different time points. That is, at baseline (prior to Mn administration), at the Mn-1 time point (33 weeks after initiation of Mn dosing; 206.4 mg Mn/kg body weight; 1216 mg Mn total dose), and at the Mn-2 time point (80 weeks after initiation of Mn dosing; 512.0 mg Mn/kg body weight; 3215.4 mg Mn total dose). The [$^{11}$C]-FLB457 time-activity curves in the frontal cortex with no AMPH and with AMPH challenge are depicted for each of the time points in the same animal (Mn3) (graphs on right side of Fig. 1). The time-activity curves in the frontal cortex with no AMPH and with AMPH challenge at baseline show that the AMPH dose produced a significant release of endogenous dopamine that was able to displace the [$^{11}$C]-FLB457 binding to D2R; thus, lowering the amount of [$^{11}$C]-FLB457 uptake in the frontal cortex. The difference between the PET scan without AMPH and the PET scan with AMPH (shaded areas in time-activity curves in right of Fig. 1) represents the amount of dopamine that was released at frontal cortex dopaminergic terminals. When one examines the differences in the [$^{11}$C]-FLB457 time-activity curves at the Mn-1 and Mn-2 time points for the same animal, there is a progressive decrease in the [$^{11}$C]-FLB457 uptake difference (shaded area in Fig. 1 time-activity curves) at the Mn-1 and Mn-2 time points compared to baseline (before Mn administration). These findings indicate that the amount of dopamine released by the AMPH dose was significantly less after the chronic Mn exposure at the Mn-1 and Mn-2 time points relative to baseline indicating an inhibitory effect of Mn on frontal cortex DAR. The data indicate that in the Mn-exposed animal, the Mn exposure resulted in a marked inhibition of percent DAR in the frontal cortex from 54.3 (baseline) to 36.2 (Mn-1) and 16.8 percent release at Mn-2 (See Fig. 2).

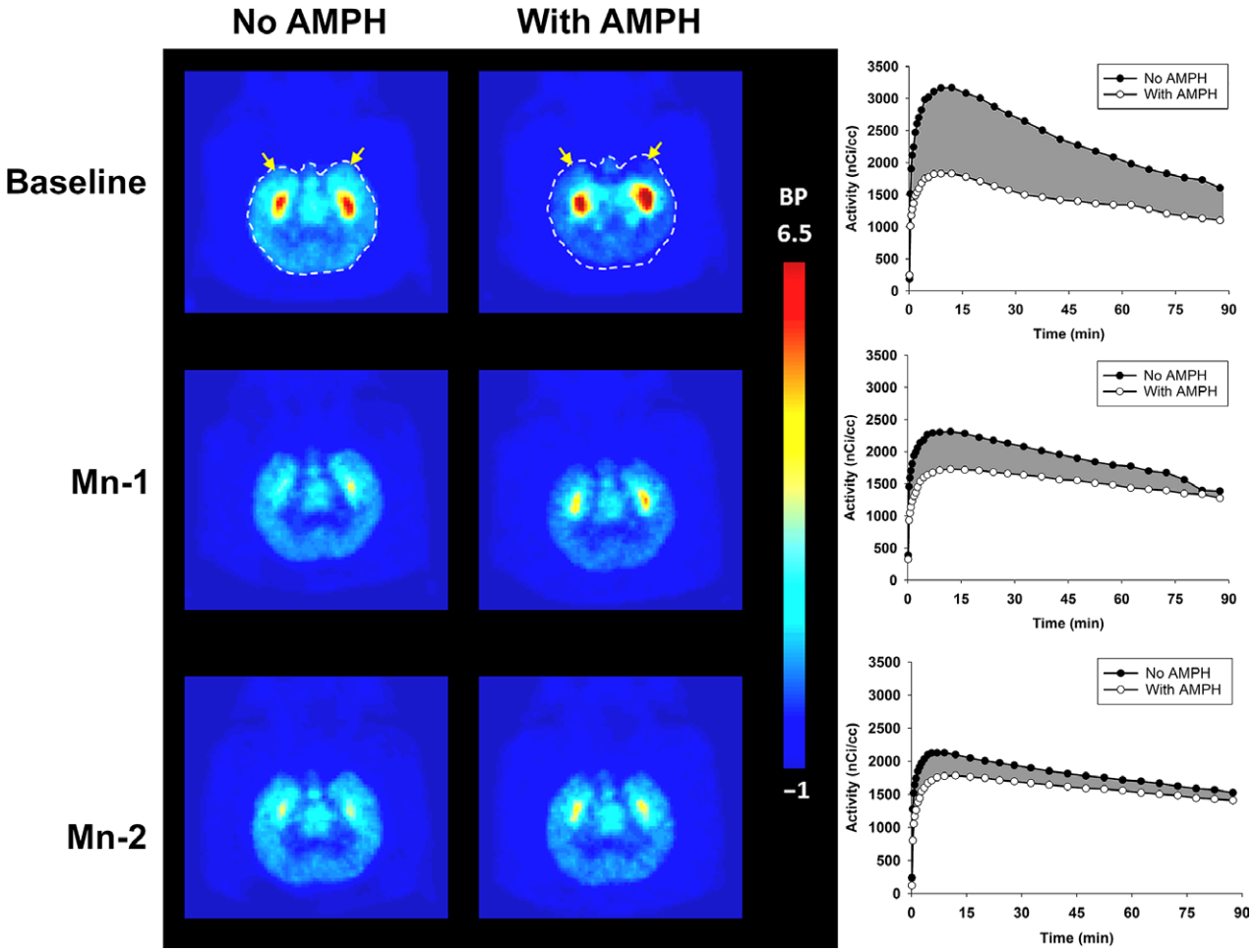


**Fig. 1** *In vivo* dopamine release in the frontal cortex of Mn-exposed non-human primates. [$^{11}$C]-FLB457 positron emission tomography with amphetamine (AMPH) challenge in the frontal cortex of the same Mn-exposed animal (Mn3) at baseline (prior to Mn exposure) and at two time points (Mn-1 and Mn-2) after the initiation of Mn exposure. In the left side of the figure, there are representative transaxial images of [$^{11}$C]-FLB457 uptake in the frontal cortex (yellow arrows) and the brain is outlined by the dashed lines. The images show that the amount of [$^{11}$C]-FLB457 uptake is significantly decreased in the baseline image with AMPH than in the baseline image with no AMPH. This effect is observed because acute AMPH administration (2 mg/kg body weight) results in a massive release of dopamine that competes with [$^{11}$C]-FLB457 for D2-dopamine receptors producing a displacement of [$^{11}$C]-FLB457 uptake from the frontal cortex. In the [$^{11}$C]-FLB457 transaxial images at the Mn-1 and Mn-2 time points there is a progressive decrease in the ability of AMPH to release dopamine indicative of a decrease in AMPH-induced dopamine release. The time-activity curves of [$^{11}$C]-FLB457 uptake in the frontal cortex in the right side of the figure confirms that the progressive accumulation of Mn in the frontal cortex results in a significant impairment AMPH-induced dopamine release. The shaded areas in the [$^{11}$C]-FLB457 time-activity curves demonstrate increased inhibition of dopamine release with progressive Mn accumulation in the frontal cortex. The time-activity curve with the solid black dots is from the striatum and the time-activity curve with the open white dots is from the cerebellum. The cerebellum is used as background or nonspecific binding since the number of D2-dopamine receptors is almost non-detectable. The time-activity curves show that with the progressive accumulation of Mn in the frontal cortex, there is a decrease in the time-activity curve with no AMPH while the time-activity curve with AMPH remains constant.

Figure 2 provides the results for all six Mn-exposed animals. The results indicate that in four of the six animals (Mn3, Mn4, Mn6, and Mn11), chronic Mn exposure resulted in a marked inhibition of frontal cortex DAR at the Mn-1 time point relative to their own baseline and a near significant effect at the Mn-2 time point although all values at Mn-2 were lower than baseline for each animal. In two Mn-exposed animals, the results were different. In one Mn-exposed animal (Mn1), there was no change in DAR at any of the time points measured and in a second animal (Mn 9) there was an increase in DAR as a result of Mn exposure relative to baseline (Fig. 2). The between-animal absolute values for baseline DAR prior to Mn exposure exhibited a high degree of variability with absolute values ranging from 14.1 to 60.9 percent DAR. It is notable that the animal in which chronic Mn exposure resulted in increased DAR

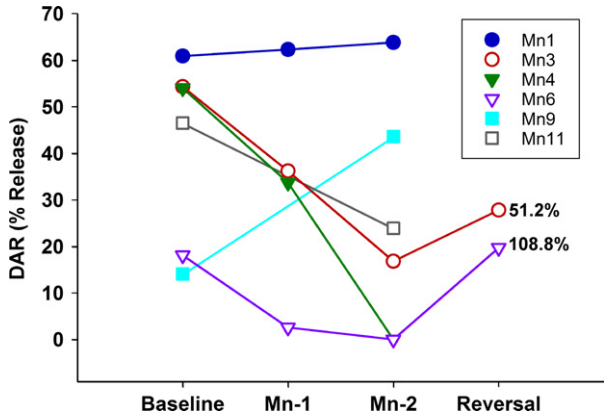


**Fig. 2** *In vivo* dopamine release in the frontal cortex of all Mn-exposed non-human primates including reversibility studies. Effect of chronic Mn exposure and cessation of exposure on *in vivo* frontal cortex dopamine release (DAR) in non-human primates. The results indicate that four animals exhibited a decrease in DAR as a function of Mn exposure (Mn3, Mn4, Mn6, and Mn11) while two animals (Mn1 and Mn9) exhibited no effect or an increase with increasing Mn exposure. Two animals (Mn3 and Mn6) in which the Mn exposure was terminated and then imaged 10 months later indicate a complete (Mn6) or partial (Mn3) reversal of Mn-induced frontal cortex DAR.

exhibited the lowest baseline DAR value while in the animal in which no effect of Mn was measured had the highest baseline DAR value (Fig. 2).

### PET imaging of frontal cortex dopamine results and behavioral endpoints

In the animals in which on average we observed a decrease in frontal cortex DAR with increasing time of Mn exposure (Fig. 3a), we observed increased attentional problems over time, as measured by reaction time in a 5-choice serial reaction time (Fig. 3b). Interestingly, the two animals that showed no change in DAR or an increase in DAR over time (Fig. 3d) performed this behavior at baseline levels at the Mn-2 time point (Fig. 3e). Similarly, spatial working memory performance decreased over time in the four animals with decreased DAR over the Mn exposure period (Fig. 3c), whereas spatial working memory remained at baseline performance at the Mn-2 time point in the two animals with unchanged or increased DAR over the Mn exposure period (Fig. 3f). It should be noted that as previously described by us, control animals showed improved performance over time (Schneider *et al.* 2015) in both tasks. One of the limitations of these associations of frontal cortex DAR and behavioral endpoints is the small number of animals. However, overall, it appears that at least, the two animals that expressed little to no change in working memory or attention performance did not exhibit a decrease in percent DAR in the frontal cortex. On the other hand, the four Mn-exposed animals that exhibited a decrease in frontal cortex DAR expressed impaired performance in either, attention, working memory, or both.

In order to begin to investigate the source of these differences, we examined the possibility that the two animals in which chronic Mn exposure did not inhibit frontal cortex DAR or attention and spatial working memory deficits may have been attributed to a lower level of Mn exposure, blood Mn concentration, or brain Mn concentration based on T1-weighted MRI relaxation time. The data in Table 2 indicate that these two animals (Mn1 and Mn9) were exposed to cumulative Mn doses similar to the other four Mn-exposed animals. Therefore, it is unlikely that Mn dosing was a contributor to the differences in these two animals relative to the rest. We also compared blood Mn concentrations at baseline and at the end of the chronic Mn exposure period (Mn-2). The data in Table 2 show that in fact blood Mn concentrations at baseline for Mn1 and Mn9 were within the range of the other four Mn-exposed animals. Therefore, blood Mn levels are unlikely to explain the lack of Mn inhibition on DAR and impairment of cognitive performance in these two animals. Finally, we examined the change in frontal cortex T1-relaxation time of Mn1 and Mn9 from baseline to Mn-2 and compared it to the other four Mn-exposed animals. Table 2 shows that the percent decrease in frontal cortex T1 relaxation time was on average 50% less for Mn1 and Mn9 than the four other Mn-exposed animals suggesting that despite the fact that Mn1 and Mn9 received a similar cumulative Mn dose and had similar blood Mn concentrations, the amount of Mn that actually reached and accumulated in the brain based on T1-weighted MRI was significantly less than in the Mn-exposed animals that expressed impaired frontal cortex DAR. This data suggest the possibility that Mn1 and Mn9 may express Mn transporters that eliminate the Mn from the brain more efficiently than the other four animals and thus may have reduced the neurotoxicological effect of Mn on DAR and behavior in these two animals. However, there should be caution in this interpretation as the findings are only from two animals. Nevertheless, the findings suggest that genetic differences between individual subjects may modulate the pharmacokinetics of Mn and thus its neurotoxicity. Future studies in humans are needed to corroborate these preliminary findings.

### Reversibility of frontal cortex Mn-induced dopamine release (DAR) deficits and Mn concentrations measured by T1-weighted MRI

We examined the possible reversibility of Mn effects on frontal cortex DAR and the elimination of Mn from the brain in two (Mn3 and Mn6) of the four Mn-exposed animals that exhibited DAR impairment measured by PET. The results show that DAR release in one animal was completely normalized to baseline levels (Mn6) while in the second animal (Mn3) there was approximately 50% recovery from

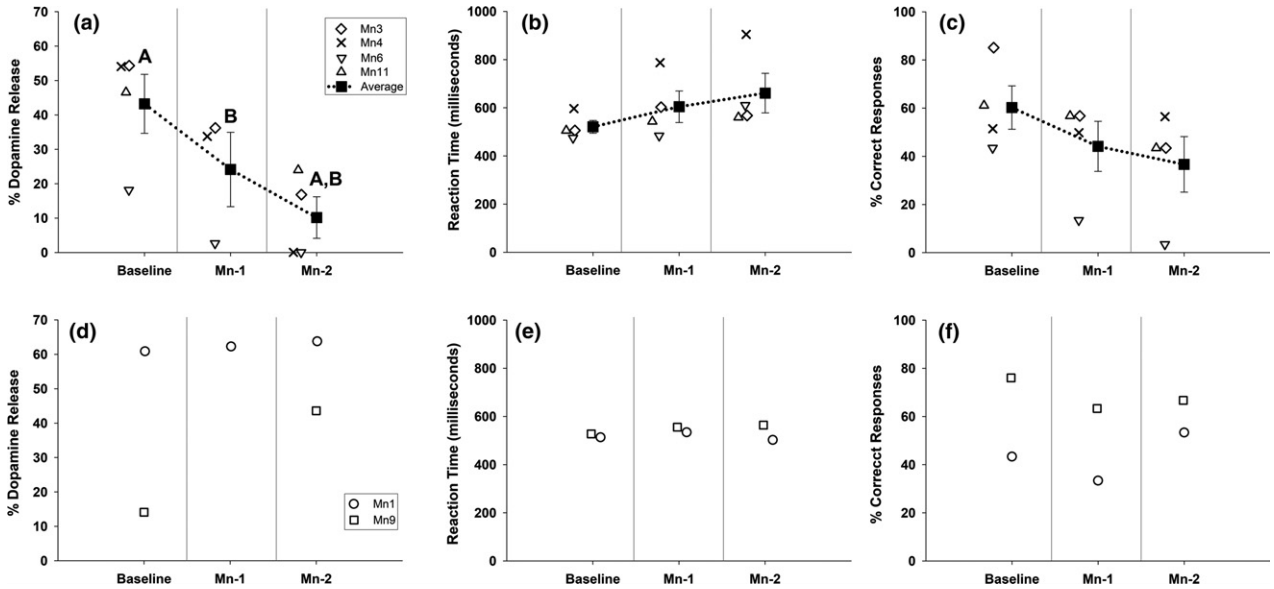


**Fig. 3** Effect of chronic Mn exposure on *in vivo* dopamine release in the frontal cortex of non-human primates and associated attention and working memory performance. (a–c) represent the findings from four Mn-exposed animals (Mn3, Mn4, Mn6, and Mn11) in which there was Mn-induced inhibition of frontal cortex dopamine release (a) [Repeated Measures ANOVA with Bonferroni Correction ($F_{2,6}$) = 12.76; $p$ = 0.007]. These animals also expressed higher reaction time scores, that is, attention (b) [nonparametric Friedman's ANOVA with Bonferroni adjustment; $p > 0.017$] and lower scores in working memory performance (c) [nonparametric Friedman's ANOVA with Bonferroni adjustment; $p > 0.017$]. Panels D-F represent the findings from two Mn-exposed animals (Mn1 and Mn9) in which there was no change or an increase in frontal cortex dopamine release (d). These animals did not express an effect of chronic Mn exposure on attention (e) or working memory (f) performance. Working memory performance was based on the most difficult level using four boxes. Average values in (a) and (b) are the mean ± SEM of 3–4 animals.

baseline 10 months after the termination of exposure to Mn (Fig. 2). It should be noted that despite the apparent recovery in DAR, animal Mn6 showed no improvement in cognitive function.

### T1-weighted MRI imaging

T1-weighted MRI imaging showed a pattern of Mn accumulation consistent with other non-human primate and human studies (Fig. 4a). Frontal cortex T1 relaxation time decreased during the Mn exposure period relative to baseline (Fig. 4b) and in the two Mn-exposed animals in which reversibility studies were performed, T1 relaxation time values returned slightly above baseline levels 10 months after Mn exposure cessation (Fig. 4b). T1 relaxation time values were inversely associated with blood Mn concentrations (compare Fig. 4b and c). These findings indicate that brain Mn concentrations normalize at 10 months of cessation of Mn exposure.

### D1R quantitative receptor autoradiography

Frontal cortex D1R plays an important role in working memory (Arnsten *et al.* 1994; Abi-Dargham *et al.* 2002). Thus, we performed D1R quantitative receptor autoradiography in postmortem frontal cortex tissue from the same animals described above and compared them to control animals not exposed to Mn. Using the D1R ligand [$^3$H]-SCH23339, we used the entire gray matter from each frontal cortex section as a global value for D1R levels in the frontal cortex. Table 3 shows that the specific binding of [$^3$H]-SCH23339 to D1R in the frontal cortex gray matter remains the same in control (23.7 ± 1.5 fmol/mg protein; $n$ = 5) and Mn-exposed animals (22.7 ± 1.22 fmol/mg tissue; $n$ = 3). There was no significant difference between control and Mn-exposed animals ($t$-test $p$ = 0.261). However, the two Mn-exposed animals that experienced cessation of Mn exposure expressed values lower than the two other groups; that is, 13.6 and 14.5 fmol/mg tissue (Table 3).

## Discussion

The main finding of this study is that chronic exposure to levels of Mn that disrupt attention and working memory performance (Schneider *et al.* 2006, 2009, 2015), results in a marked inhibition of frontal cortex DAR. Parenthetically, in previous studies, we have also shown that a similar Mn exposure paradigm inhibits DAR in the striatum using [$^{11}$C]-raclopride PET (Guilarte *et al.* 2006, 2008a). In the current study, one Mn-exposed animal that had the highest absolute DAR value (Mn1) at baseline, chronic Mn exposure did not have an effect on DAR at any of the time points measured

**Table 2** Analysis of Mn1 and Mn9 animals relative to Mn3, Mn4, Mn6, and Mn11 at baseline and at end of chronic manganese exposure

| Measured endpoints | Baseline | Mn-2 |
|---|---|---|
| Cumulative Mn (mg/kg) | | |
| Mn3, Mn4, Mn6, Mn11 | 0 ($n$ = 4) | 512.0, 517.2, 421.0, 375.5<br>456.4 ± 34.9 ($n$ = 4) |
| Mn1, Mn9 | 0 ($n$ = 2) | 511.9, 382.0<br>447.0 ($n$ = 2) |
| Blood Mn levels (μg/L) | | |
| Mn3, Mn4, Mn6, Mn11 | 19.7, 9.5, 8.9, 3.5<br>10.4 ± 3.4 ($n$ = 4) | 83.2, 139.6, 121.2, 122.3<br>116.6 ± 11.9 ($n$ = 4) |
| Mn1, Mn9 | 6.3, 4.1<br>5.2 ($n$ = 2) | 84.9, 99.4<br>92.2 ($n$ = 2) |
| Frontal cortex T1 relaxation times (ms) | | |
| Mn3, Mn4, Mn6, Mn11 | 874.4, 1034.1, 911.8, 837.4 | 693.8 (−19.8%), 923.2 (−10.7%), 755.7 (−17.1%), 741.6 (−11.4%) |
| | 914.4 ± 42.7 ($n$ = 4) | 778.6 ± 50.0 ($n$ = 4) (−15.0%) |
| Mn1, Mn9 | 907.7, 942.8 | 827.5 (−8.8%), 894.5 (−5.1%) |
| | 925.3 ($n$ = 2) | 861.0 ($n$ = 2) (−7.0%) |

The percent in parenthesis for T1 relaxation time results at Mn-2 time point represents the percent decrease in T1 relaxation time in the frontal cortex from baseline value. Data are mean values ± SEM.

(Fig. 2). Further, in another Mn-exposed animal (Mn9), that had the lowest absolute level of frontal cortex DAR at baseline, chronic Mn exposure actually increased frontal cortex DAR relative to its own baseline (Fig. 2). It is notable that these two animals exhibited the highest and lowest frontal cortex DAR absolute values at baseline relative to the other four animals in which frontal cortex DAR was inhibited by chronic Mn exposure. While we currently do not have an explanation for the deviation of these two Mn-exposed animals from the four animals in which Mn exposure impaired DAR and behavior, the T1 relaxation time data indicate that despite similar cumulative Mn doses administered and blood Mn concentrations, T1 relaxation time percent change from baseline was less in Mn1 and M9 than the other four animals (Table 2). This finding, although preliminary, suggests that a lower level of Mn accumulated in the frontal cortex of Mn1 and Mn9. It may also provide a potential explanation for the differences in neurotoxicity observed in these two Mn-exposed animals relative to the four other animals in which inhibition of DAR and impairment of working memory and attention were found. Furthermore, our present finding may be relevant to a recent human study in which common non-coding single-nucleotide polymorphism of the *SLC30A10* gene, a putative Mn transporter, alters neurological function independent of blood Mn concentrations (Wahlberg *et al.* 2016). Combined, these findings suggest the possibility that brain Mn concentrations may depend on common *SLC30A10* gene variants that modulate Mn neurotoxicity.

Other studies suggest that DAR and working memory performance are influenced by initial levels of dopamine in the frontal cortex or dopaminergic tone in frontal cortex neurons (Brozoski *et al.* 1979; Vijayraghavan *et al.* 2007; Cools and D'Esposito 2011; Clark and Noudoost 2014). Importantly, baseline spatial working memory performance of Mn1 and Mn9 was not substantially different from that of the other animals (data not shown) despite having significantly different DAR absolute values. These findings suggest the possibility that other neuronal systems besides the dopaminergic system may also contribute to the deficits in working memory performance and attention as a result of chronic Mn exposure.

We also examined the potential for reversibility of Mn-induced impairment of frontal cortex DAR after 10 months from the last Mn dose. We found that in one animal (Mn3) there was complete recovery of DAR relative to baseline while in the second animal (Mn6) there was partial recovery (approximately 51%; Fig. 2). As indicated in the results section, in Mn3 despite a complete recovery of DAR, the working memory performance of this animal remained impaired. Thus, injury or dysfunction of other neuronal systems besides dopamine is likely to be involved. We should note that while Mn-induced impairment of DAR also occurs in the striatum (Guilarte *et al.* 2006, 2008a), we have not determined if it is reversible in this brain region. This type of data could provide valuable mechanistic information about the potential for reversibility of Mn neurotoxicity in different brain regions and provide insights on putative pathophysiological mechanisms.

Previous human and animal studies have shown that increasing or decreasing dopamine levels in the frontal cortex impairs working memory performance (Brozoski *et al.* 1979; Vijayraghavan *et al.* 2007; Cools and D'Esposito 2011; Clark and Noudoost 2014), and frontal cortex dopamine modulates working memory via D1R activation (Arnsten *et al.* 1994; Takahashi *et al.* 2012;). D1R modulation of working memory follows an inverted U-shaped curve, where an optimal level of D1R activation is required for optimal performance and too much or too little activation of D1R degrades working memory performance (Watanabe *et al.* 1997; Zahrt *et al.* 1997; Vijayraghavan *et al.* 2007; Cools and D'Esposito 2011; Clark and Noudoost 2014). It is possible that a similar effect is occurring in Mn-exposed animal where Mn-induced increased or decreased DAR in the frontal cortex is based on baseline DAR levels. Our current findings of a Mn-induced inhibition of frontal cortex DAR along with our previous results of Mn-induced inhibition of DAR in the striatum (Guilarte *et al.* 2006,

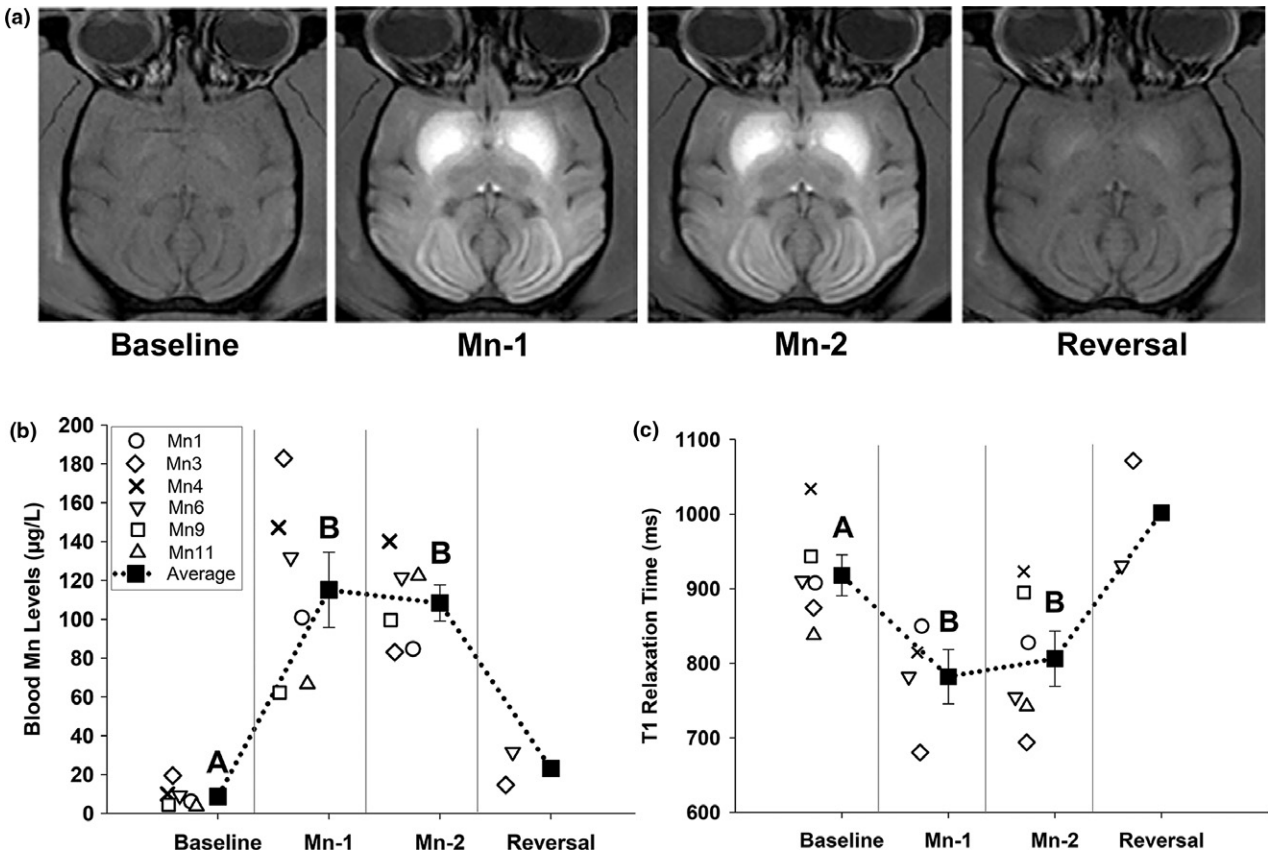


**Fig. 4** T1-weighted magnetic resonance imaging (MRI) imaging of Mn-exposed non-human primates. (a) T1-weighted MRI of the frontal cortex in the same Mn-exposed monkey (Mn-3) over time. (a) shows the T1-weighted MRI of the same monkey before (baseline), during Mn exposure (Mn-1 and Mn-2) and after 10 months of cessation of Mn exposure (reversal). The chronic Mn exposure resulted in an overall increase in Mn accumulation in the entire brain as depicted by the increased hyperintensive signal during the Mn exposure period relative to baseline. There was complete elimination of Mn from the brain after 10 months of cessation of Mn exposure. (b) depicts the frontal cortex T1 relaxation times as a function of exposure for all six animals. The T1 relaxation time was significantly decreased during Mn exposure relative to baseline in all animals [Repeated measures ANOVA with Bonferroni correction ($F_{2,10}$) = 15.96; $p$ = 0.001]. (c) depicts the blood Mn concentration of all six animals during the different periods of the study. There was a highly significant increase in blood Mn concentrations at the Mn-1 and Mn-2 time points relative to baseline [Repeated measures ANOVA with Bonferroni correction ($F_{2,10}$) = 23.98; $p < 0.001$). The blood Mn concentration was associated with increased Mn deposition in the brain and T1 relaxation times in the frontal cortex. Average values in (b) and (c) are the mean ± SEM of 4–6 animals. For (b) and (c), groups with different letters are significantly different at $p < 0.05$ (Bonferroni correction $p < 0.017$).

2008a) may help explain the impairments in attention and working memory documented in Mn-exposed non-human primates exposed to similar levels of Mn (Schneider *et al.* 2006, 2009, 2015). However, it is highly likely that other neuronal systems are also involved. For example, the cholinergic system in the prefrontal cortex modulates neuronal firing during a working memory task (Sun *et al.* 2017) and there is evidence that cholinergic function is affected by chronic Mn exposure (Finkelstein *et al.* 2007).

Frontal cortex D1R levels modulate working memory performance (Sawaguchi and Goldman-Rakic 1991). Therefore, we performed [$^3$H]-SCH23399 quantitative receptor autoradiography to assess D1R levels in postmortem frontal cortex tissue from the same animals. Our findings indicate that Mn-exposed animals that did not experience elimination of Mn from the brain expressed D1R receptor levels similar to controls (Table 3). Notably, the animals that experienced elimination of Mn from the brain (i.e., reversal animals) expressed frontal cortex D1R levels that were approximately 50–60% of naïve controls and Mn-exposed animals that did not experience reversibility. Frontal cortex D1R did not differ between non-exposed control animals and Mn-exposed animals without reversibility (Table 3). One potential interpretation of the results in the Mn-exposed animals that experienced reversibility is that the elimination of Mn from the brain, increased DAR and thus synaptic levels of dopamine with a putative down-regulation of D1R. This interpretation is consistent with the fact that DAR increased

**Table 3** D1-dopamine receptor quantitative autoradiography in the frontal cortex of Mn-exposed and non-exposed control animals

| Treatment | Animal ID | [$^3$H]-SCH23339 specific binding (fmol/mg tissue) | |
|---|---|---|---|
| Control ($n$ = 5) | Mn2, Mn5, Mn7, Mn13, Mn14 | 23.7 ± 1.5 | 20.8, 28.7, 19.7, 24.5, 25.2 |
| Mn ($n$ = 3) | Mn4, Mn9, Mn11 | 22.7 ± 1.2 | 22.6, 24.9, 20.7 |
| Mn + reversal ($n$ = 2) | Mn3, Mn6 | 14.0 | 13.6, 14.5 |

Data are mean values ± SEM.

in both Mn-exposed animals that experienced reversal (Fig. 2).

Previous studies from our laboratory have shown significant frontal cortex pathology in animals exposed to similar level of Mn as in the present study. For example, postmortem studies in the frontal cortex of Mn-exposed non-human primates have found a significant degree of neuronal degeneration with diffused β-amyloid plaques and α-synuclein aggregation (Guilarte *et al.* 2008b; Verina *et al.* 2013) implicating a potentially important role of this frontal cortex neuropathology in the working memory and attention deficits observed in Mn-exposed non-human primates (Schneider *et al.* 2009, 2015). Collectively, our previous and present studies provide significant experimental evidence that chronic exposure to moderate levels of Mn impairs nigrostriatal and mesocortical dopaminergic neurotransmission and produces pathologies in brain structures such as the frontal cortex that are important for attention and working memory performance.

As previously noted, one limitation of the present study is the number of animals that were studied. Despite their limitations, the present results provide significant and valuable information that chronic Mn exposure alters the dopaminergic mesocortical system and provides evidence of some degree of reversibility of Mn inhibition of DAR in the frontal cortex. Furthermore, our findings suggest that while the dopaminergic system is likely to be involved in the working memory and attention deficits observed in Mn-exposed animals and humans, effects on the dopaminergic system alone do not fully explain the cognitive function deficits and other neuronal systems are also likely to be involved.

Our present findings in non-human primates support other studies in Mn-exposed humans. That is, humans chronically exposed to Mn exhibit deficits in working memory and pathological changes in brain structures relevant to working memory. For example, imaging studies in smelter workers exposed to Mn support a Mn-induced neuronal cell death or dysfunction in the frontal cortex based on decreased *N*-acetylaspartate/total creatine ratio measured by magnetic resonance spectroscopy (Dydak *et al.* 2011), an effect that was associated with cumulative Mn exposure. A decrease in the *N*-acetylaspartate/total creatine ratio is indicative of neuronal degeneration and/or dysfunction.

Other studies report that welders with chronic Mn exposure express increased brain activity measured by functional MRI in working memory networks during the 2-back verbal working memory task (Chang *et al.* 2010). The authors interpret these findings as the welders requiring more neural resources in working memory networks to compensate for deficits in working memory. Stepens *et al.* (2010) have shown that individuals injecting the Mn-containing psychostimulant drug ephedrone express white matter abnormalities based on diffusion tensor imaging. They describe evidence of diffuse white matter changes reflected by reductions in fractional anisotropy (FA) in ephedrone users. These effects were specific to white matter underlying the right ventral premotor cortex and the medial prefrontal cortex. They indicate that the clinical features of these Mn-containing ephedrone users point to a disorder of higher-level motor programming and that the pattern of motor function deficits resembles executive function deficits similar to those displayed by patients with prefrontal cortex lesions (Stepens *et al.* 2010). Another human study examining white matter ultrastructural integrity in Mn-exposed welders revealed white matter changes measured by diffusion tensor imaging (Kim *et al.* 2011). They show that FA was significantly reduced in the corpus callosum and frontal white matter in welders. Importantly, the degree of FA disruption was associated with impaired attention, lower working memory, and deficits in executive function tests (Kim *et al.* 2011).

Finally, Juurmaa *et al.* (2016) report that methcathinone (ephedrone) abusers exhibit widespread structural and functional changes affecting cortical and subcortical gray matter and their connections. Specifically, bilateral reductions of putamen and thalamus volume and right caudate nucleus with cortical thinning. Using resting state functional MRI they also found significantly increased bilateral functional connectivity in methcathinone (ephedrone) abusers within the primary motor cortex. The authors note that the most consistent site of gray matter loss was in the putamen and this effect was associated with motor symptomatology.

In summary, while the underlying neurochemistry and neuropathology of Mn neurotoxicity in the frontal cortex is by no means complete, the present work and other non-human primate and human studies provide significant evidence that cognitive domains mediated by the working memory network and the modulatory role of the dopaminergic system in frontal cortex and fronto-striatal circuits are significantly altered by chronic Mn exposure. Furthermore, dysfunction of other neuronal systems such as the cholinergic system may also contribute to the cognitive function deficits. Finally, it is interesting to note that one of the early clinical symptoms of high Mn exposure in humans is psychosis

(Chandra 1983; Donaldson 1987; Chamelian *et al.* 2018) and a recent human study using [$^{11}$C]-FLB457 PET shows impairment of DAR in the dorsolateral prefrontal cortex of schizophrenia subjects (Silfstein *et al.* 2015). It is possible that the inhibition of frontal cortex DAR by chronic Mn exposure may also form the basis for some of the psychiatric symptoms observed in Mn-intoxicated subjects.

## Acknowledgments and conflict of interest disclosure

This work was funded by a grant from the National Institute of Environmental Health Sciences ES010975 to TRG. The authors have no conflicts of interest to report. We wish to thank Dr. Changwon Yoo for statistical consultation.

All experiments were conducted in compliance with the ARRIVE guidelines.

## References

Aalto S., Bruck A., Laine M., Nagren K. and Rinne J. O. (2005) Frontal and temporal dopamine release during working memory and attention tasks in healthy humans: a positron emission tomography study using the high-affinity dopamine D2 ligand [$^{11}$C]FLB 457. *J. Neurosci.* **25**, 2471–2477.

Abi-Dargham A., Mawlawi O., Lombardo I. *et al.* (2002) Prefrontal dopamine D1 receptors and working memory in schizophrenia. *J. Neurosci.* **22**, 3708–3719.

Alexander G. E., DeLong M. R. and Strick P. L. (1986) Parallel organization of functionally segregated circuits linking basal ganglia and cortex. *Ann. Rev. Neurosci.* **9**, 357–381.

Arnsten A. F., Cai J. X., Murphy B. L. and Goldman-Rakic P. S. (1994) Dopamine D1 receptor mechanisms in the cognitive performance of young adult and aged monkeys. *Psychopharmacology* **116**, 143–151.

Berman K. F., Ostrem J. L., Randolph C., Gold J., Goldberg T. E., Coppola R., Carson R. E., Herscovitch P. and Weinberger D. R. (1995) Physiological activation of a cortical network during performance of the Wisconsin Card Sorting Test: a positron emission tomography study. *Neuropsychologia* **33**, 1027–1046.

Bjorklund A. and Dunnett S. B. (2007) Dopamine neuron systems in the brain: an update. *Trends Neurosci.* **30**, 194–202.

Bouchard M., Mergler D., Baldwin M., Panisset M. and Roels H. A. (2007) Neuropsychiatric symptoms and past manganese exposure in a ferro-alloy plant. *Neurotoxicology* **28**, 290–297.

Bowler R. M., Gysens S., Diamond E., Booty A., Hartney C. and Roels H. A. (2003) Neuropsychological sequelae of exposure to welding fumes in a group of occupationally exposed men. *Int. J. Hyg. Env. Hlth.* **206**, 517–529.

Bowler R. M., Gysens S., Diamond E., Nakagawa S., Drezgic M. and Roels H. A. (2006) Manganese exposure: neuropsychological and neurological symptoms and effects in welders. *Neurotoxicology* **27**, 315–326.

Bowler R. M., Roels H. A., Nakagawa S. *et al.* (2007a) Dose-effect relationships between manganese exposure and neurological, neuropsychological and pulmonary function in confined space bridge welders. *Occup. Environ. Med.* **64**, 167–177.

Bowler R. M., Nakagawa S., Drezgic M., Roels H. A., Park R. M., Diamond E., Mergler D., Bouchard M., Bowler R. P. and Koller W. (2007b) Sequelae of fume exposure in confined space welding: a neurological and neuropsychological case series. *Neurotoxicology* **28**, 298–311.

Brozoski T. J., Brown R. M., Rosvold H. E. and Goldman P. S. (1979) Cognitive deficits caused by regional depletion of dopamine in prefrontal cortex of rhesus monkey. *Science* **205**, 929–932.

Chalela J. A., Bonilha L., Neyens R. and Hayes A. (2010) Manganese encephalopathy: an under recognized condition in intensive care unit. *Neurocrit. Care* **14**, 456–458.

Chamelian L., Pereira A., Grant K. and Maurice C. (2018) Case report: atypical neuropsychiatric presentation in a patient expecting liver transplantation. *Case Rep. Transplant.* **2018**, 1–3.

Chandra S. V. (1983) Psychiatric illness due to manganese poisoning. *Acta Psychiatr. Scand. Suppl.* **303**, 49–54.

Chang Y., Lee J. J., Seo J. H. *et al.* (2010) Altered working memory process in the manganese-exposed brain. *NeuroImage* **53**, 1279–1285.

Clark K. L. and Noudoost B. (2014) The role of prefrontal catecholamines in attention and working memory. *Front. Neural. Circuits.* **8**, 33.

Cohen J. D., Perlstein W. M., Braver T. S., Nystrom L. E., Noll D. C., Jonides J. and Smith E. E. (1997) Temporal dynamics of brain activation during a working memory task. *Nature* **386**, 604–608.

Constantinidis C. and Wang X. J. (2004) A neural basis for working memory. *Neuroscientist* **10**, 553–565.

Cools R. and D'Esposito M. (2011) Inverted-U-shaped dopamine actions on human working memory and cognitive control. *Biol. Psych.* **69**, e113–e125.

Donaldson J. (1987) The physiopathologic significance of manganese in brain: its relation to schizophrenia and neurodegenerative disorders. *Neurotoxicology* **8**, 451–462.

Dydak U., Jiang Y.-M., Long L.-L. *et al.* (2011) *In vivo* measurement of brain GABA concentrations by magnetic resonance spectroscopy in smelters occupationally exposed to manganese. *Environ. Health Perspect.* **119**, 219–224.

Finkelstein Y., Milatovic D. and Aschner M. (2007) Modulation of cholinergic systems by manganese. *Neurotoxicology* **28**, 1003–1014.

Guilarte T. R. (2010) Manganese and Parkinson's disease: a critical review and new findings. *Environ. Health Perspect.* **118**, 1071–1080.

Guilarte T. R. (2013) Manganese neurotoxicity: new perspectives from behavioral, neuroimaging, and neuropathological studies in humans and non-human primates. *Front. Aging Neurosci.* **5**, 23.

Guilarte T. R. and Gonzales K. K. (2015) Manganese-induced parkinsonism is not idiopathic Parkinson's disease: environmental and genetic evidence. *Toxicol. Sci.* **146**, 204–212.

Guilarte T. R., Chen M. K., McGlothan J. L. *et al.* (2006) Nigrostriatal dopamine system dysfunction and subtle motor deficits in manganese-exposed non-human primates. *Exp. Neurol.* **202**, 381–390.

Guilarte T. R., Burton N. C., McGlothan J. L. *et al.* (2008a) Impairment of nigrostriatal dopamine neurotransmission by manganese is mediated by pre-synaptic mechanism(s): implications to manganese-induced parkinsonism. *J. Neurochem.* **107**, 1236–1247.

Guilarte T. R., Burton N. C., Verina T., Prabhu V. V., Becker K. G., Syversen T. and Schneider J. S. (2008b) Increased APLP1 expression and neurodegeneration in the frontal cortex of manganese-exposed non-human primates. *J. Neurochem.* **105**, 1948–1959.

Jedema H. P., Narenderan R. and Bradberry C. W. (2014) Amphetamine-induced release of dopamine in primate prefrontal cortex and striatum: striking differences in magnitude and timecourse. *J. Neurochem.* **130**, 490–497.

Jokinen P., Karrash M., Bruck A., Johansson J., Bergman J. and Rinne J. O. (2013) Cognitive slowing in Parkinson's disease is related to frontostriatal dopaminergic dysfunction. *J. Neurol. Sci.* **329**, 23–28.

Josephs K. A., Ahlskog J. E., Klos K. J., Kumar N., Fealey R. D., Trenerry M. R. and Cowl C. T. (2005) Neurologic manifestations in welders with pallidal MRI-T1 hyperintensity. *Neurology* **64**, 2033–2039.

Juurmaa J., Menke R. A., Vila P. *et al.* (2016) Grey matter abnormalities in methcathinone abusers with a parkinsonian syndrome. *Brain Behav.* **6**, e00539.

Kim Y., Jeong K. S., Song H. J. *et al.* (2011) Altered white matter microstructural integrity revealed by voxel-wise analysis of diffusion tensor imaging in welders with manganese exposure. *Neurotoxicology* **32**, 100–109.

Klos K. J., Chandler K., Kumar N., Ahiskog J. E. and Josephs K. A. (2006) Neuropsychological profiles of manganese neurotoxicity. *Eur. J. Neurol.* **13**, 1139–1141.

Laruelle M. (2000) Imaging synaptic neurotransmission with in vivo binding competition techniques: a critical review. *J. Cereb. Blood Flow Metab.* **20**, 423–451.

Linden D. E. (2007) The working memory networks of the human brain. *Neuroscientist* **13**, 257–267.

Mackenzie Ross S. (2018) Delayed cognitive and psychiatric symptoms following methyl iodide and manganese poisoning: potential for misdiagnosis. *Cortex* **74**, 427–439.

Mergler D. and Baldwin M. (1997) Early manifestations of manganese neurotoxicity in humans: an update. *Environ. Res.* **73**, 90–104.

Mergler D., Baldwin M., Belanger S. *et al.* (1999) Manganese neurotoxicity, a continuum of dysfunction: results form a community based study. *Neurotoxicology* **20**, 327–342.

Mirowitz S. A., Westrich T. J. and Hirsch J. D. (1991) Hyperintensive basal ganglia on T1-weighted MR images in patients receiving parenteral nutrition. *Radiology* **181**, 117–120.

Narendran R., Frankle W. G., Mason N. S. *et al.* (2009) Positron emission tomography imaging of amphetamine-induced dopamine release in the human cortex: a comparative evaluation of the high affinity dopamine D2/D3 radiotracers [$^{11}$C]-FLB 457 and [$^{11}$C]-Fallypride. *Synapse* **63**, 447–461.

Narendran R., Mason N. S., May M. A., Chen C.-M., Kendro S., Ridler K., Rabiner E. A., Laruelle M., Mathis C. A. and Frankle W. G. (2011a) Positron emission tomography imaging of dopamine D2/D3 receptors in the human cortex with [$^{11}$C]-FLB 457: reproducibility studies. *Synapse* **65**, 35–40.

Narendran R., Mason N. S., Chen C.-M., Himes M., Keating P., May M. A., Rabiner E. A., Laruelle M., Mathis C. A. and Frankle W. G. (2011b) Evaluation of dopamine D2/D3 specific binding in the cerebellum for the positron emission tomography radiotracer [$^{11}$C]-FLB 457: implications for measuring cortical dopamine release. *Synapse* **65**, 991–997.

Narendran R., Jedema H. P., Lopresti B. J., Mason N. S., Gurnsey K., Ruszkiewicz J., Chen C.-M., Deuitch L., Frankle W. G. and Bradberry C. W. (2014) Imaging dopamine transmission in the frontal cortex: a simultaneous microdialysis and [$^{11}$C]-FLB 457 PET study. *Mol. Psych.* **19**, 302–310.

Olanow C. W. (2004) Manganese-induced Parkinsonism and Parkinson's disease. *Ann. N. Y. Acad. Sci.* **1012**, 209–223.

Pal P. K., Samil A. and Calne D. B. (1999) Manganese neurotoxicity: a review of clinical features, imaging and pathology. *Neurotoxicology* **20**, 227–238.

Park R. M., Bowler R. M. and Roels H. A. (2009) Exposure-response relationships and risk assessment for cognitive deficits in early welding-induced manganism. *J. Occup. Environ. Med.* **51**, 1125–1136.

Perl D. P. and Olanow C. W. (2007) The neuropathology of manganese-induced Parkinsonism. *J. Neuropathol. Exp. Neurol.* **66**, 675–682.

Petrides M., Alivisatos B., Meyer E. and Evans A. C. (1993) Functional activation of the human frontal cortex during the performance of verbal working memory tasks. *Proc. Natl Acad. Sci. USA* **90**, 878–882.

Rinne J. O., Portin R., Ruottinen H., Nurmi E., Bergman J., Haaparanta M. and Solin O. (2000) Cognitive impairment and the brain dopaminergic system in Parkinson's disease: [18F]fluorodopa positron emission tomography study. *Arch. Neurol.* **57**, 470–475.

Roels H. A., Bowler R. M., Kim Y. *et al.* (2013) Manganese exposure and cognitive deficits: a growing concern for manganese neurotoxicity. *Neurotoxicology* **33**, 872–880.

Rotaru D. C., Lewis D. A. and Gonzalez-Burgos G. (2007) Dopamine D1 receptor activation regulates sodium channel-dependent EPSP amplification in rat prefrontal cortex pyramidal neurons. *J. Physiol.* **581**, 981–1000.

Santos-Burgoa C., Rios C., Mercado L. A., Arechiga-Serrano R., Cano-Valle F., Eden-Wynter R. A., Texcalac-Sangrador J. L., Villa-Boragar J. P., Rodriguez-Agudelo Y. and Montes S. (2001) Exposure to manganese: health effects on the general population, a pilot study in central Mexico. *Environ. Res.* **85**, 90–104.

Sawaguchi T. and Goldman-Rakic P. S. (1991) D1 dopamine receptors in prefrontal cortex: involvement in working memory. *Science* **251**, 947–950.

Sawamoto N., Piccini P., Hotton G., Pavese N., Thielemans K. and Brooks D. J. (2008) Cognitive deficits and striato-frontal dopamine release in Parkinson's disease. *Brain* **131**, 1294–1302.

Schneider J. S., Decamp E., Koser A. J., Fritz S., Gonczi H., Syversen T. and Guilarte T. R. (2006) Effects of chronic manganese exposure on cognitive and motor functioning in non-human primates. *Brain Res.* **1118**, 222–231.

Schneider J. S., Decamp E., Clark K., Bouquio C., Syversen T. and Guilarte T. R. (2009) Effects of chronic manganese exposure on working memory in non-human primates. *Brain Res.* **1258**, 86–95.

Schneider J. S., Williams C., Ault T. and Guilarte T. R. (2013) Chronic manganese exposure impairs visuospatial associative learning in non-human primates. *Toxicol. Lett.* **221**, 146–151.

Schneider J. S., Williams C., Ault M. and Guilarte T. R. (2015) Effects of chronic manganese exposure on attention and working memory in non-human primates. *Neurotoxicology* **48**, 217–222.

Seger C. A. (2006) The basal ganglia in human learning. *Neuroscientist* **12**, 285–290.

Silfstein M., van de Giessen E., Snellenberg J. V. *et al.* (2015) Deficits in prefrontal cortical and extrastriatal dopamine release in schizophrenia. A positron emission tomography functional magnetic resonance imaging study. *JAMA Psychiatry* **72**, 316–324.

Stepens A., Stagg C. J., Platkajis A., Boudrias M.-H., Johansen-Berg H. and Donaghy M. (2010) White matter abnormalities in methcathinone abusers with an extrapyramidal syndrome. *Brain* **133**, 3676–3684.

Sun Y., Yang Y., Galvin V. C., Yang S., Arnsten A. F. and Wang M. (2017) Nicotinic α4β2 cholinergic receptor influences on dorsolateral prefrontal cortical neuronal firing during a working memory task. *J. Neurosci.* **37**, 5366–5377.

Takahashi H., Yamada M. and Suhara T. (2012) Functional significance of central D1 receptors in cognition: beyond working memory. *J. Cereb. Blood Flow Metab.* **32**, 1248–1258.

Verina T., Schneider J. S. and Guilarte T. R. (2013) Manganese induces α-synuclein aggregation in the frontal cortex of non-human primates. *Toxicol. Lett.* **217**, 177–183.

Vijayraghavan S., Wang M., Birnbaum S. G., Williams G. V. and Arnsten A. F. T. (2007) Inverted U dopamine D1 receptor actions on prefrontal neurons engaged in working memory. *Nat. Neurosci.* **10**, 376–384.

Wahlberg K., Kippler M., Alhamdow A., Rahman S. M., Smith D. R., Vahter M., Lucchini R. G. and Broberg K. (2016) Common polymorphism in the Solute Carrier SLC30A10 are associated with blood manganese and neurological function. *Toxicol. Sci.* **149**, 473–483.

Watanabe M., Kodama T. and Hikosaka K. (1997) Increase of extracellular dopamine in primate prefrontal cortex during a working memory task. *J. Neurophysiol.* **78**, 2795–2798.

Zahrt J., Taylor J. R., Mathew R. G. and Arnsten A. F. (1997) Supranormal stimulation of D1 dopamine receptors in the rodent prefrontal cortex impairs spatial working memory performance. *J. Neurosci.* **17**, 8528–8535.

Zhou Y., Endres C. J., Brasic J. R., Huang S. C. and Wong D. F. (2003) Linear regression with spatial constraint to generate parametric images of ligand-receptor dynamic PET studies with a simplified reference tissue model. *NeuroImage* **18**, 975–989.

Zhou Y., Chen M.-K., Endres C. J., Ye W., Brasic J. R., Alexander M., Crabb A. H., Guilarte T. R. and Wong D. F. (2006) An extended simplified reference tissue model for the quantification of dynamic PET with amphetamine challenge. *NeuroImage* **33**, 550–563.